Exploration of Metal Chloride Uptake for Improved Performance Characteristics of PbSe Quantum Dot Solar Cells

ARTICLE *in* JOURNAL OF PHYSICAL CHEMISTRY LETTERS · JULY 2015

Impact Factor: 7.46 · DOI: 10.1021/acs.jpclett.5b01214

5 AUTHORS, INCLUDING:

Ashley R. Marshall
National Renewable Energy Laboratory
6 PUBLICATIONS **10** CITATIONS
SEE PROFILE

A. J. Nozik
University of Colorado Boulder
310 PUBLICATIONS **19,501** CITATIONS
SEE PROFILE

Matthew C Beard
National Renewable Energy Laboratory
114 PUBLICATIONS **7,874** CITATIONS
SEE PROFILE

Joseph M Luther
National Renewable Energy Laboratory
83 PUBLICATIONS **5,246** CITATIONS
SEE PROFILE

THE JOURNAL OF PHYSICAL CHEMISTRY Letters

Letter

pubs.acs.org/JPCL

Exploration of Metal Chloride Uptake for Improved Performance Characteristics of PbSe Quantum Dot Solar Cells

Ashley R. Marshall,[†,‡] Matthew R. Young,[†] Arthur J. Nozik,[†,‡] Matthew C. Beard,[†] and Joseph M. Luther*[,†]

[†]National Renewable Energy Laboratory, Golden, Colorado 80401, United States

[‡]Department of Chemistry and Biochemistry, University of Colorado, Boulder, Colorado 80309, United States

Supporting Information

ABSTRACT: We explored the uptake of metal chloride salts with +1 to +3 metals of Na^+, K^+, Zn^{2+}, Cd^{2+}, Sn^{2+}, Cu^{2+}, and In^{3+} by PbSe QD solar cells. We also compared $CdCl_2$ to Cd acetate and Cd nitrate treatments. PbSe QD solar cells fabricated with a $CdCl_2$ treatment are stable for more than 270 days stored in air. We studied how temperature and immersion times affect optoelectronic properties and photovoltaic cell performance. Uptake of Cd^{2+} and Zn^{2+} increase open circuit voltage, whereas In^{3+} and K^+ increase the photocurrent without influencing the spectral response or first exciton peak position. Using the most beneficial treatments we varied the bandgap of PbSe QD solar cells from 0.78 to 1.3 eV and find the improved V_{OC} is more prevalent for lower bandgap QD solar cells.

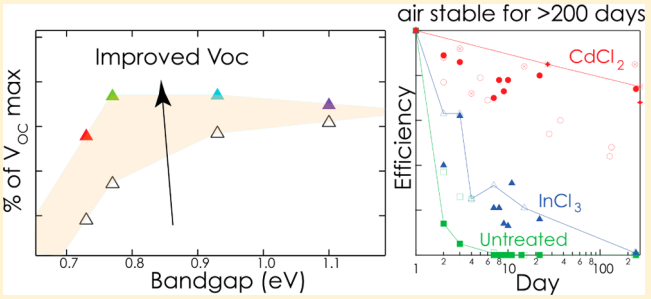

Lead chalcogenide quantum dots (QDs) are actively researched for optoelectronic devices due to unique and customizable optoelectronic features;[1,2] tunable bandgap, control over workfunction,[3,4] ease of synthesis,[5,6] and enhanced multiple exciton generation (MEG).[7−12] Colloidal solutions of PbSe QDs have been extensively explored for fundamental studies[9,13−22] and incorporated into photovoltaic, proof of principle, architectures.[7,23−30] Nevertheless, PbSe QD solar cells have received less attention than PbS QD solar cells mainly due to more problematic air stability. A common theme in PbSe QD studies involves not exposing the QDs to oxygen or water,[20,31,32] which can be accomplished within a controlled atmosphere glovebox or by encapsulating the QD films, such as by matrix infilling.[33] Recently Zhang and co-workers developed new synthetic protocols that resulted in high efficiency (5−6%) PbSe QDSCs fabricated in ambient conditions.[4,34] Despite these improvements, device characteristics still lag behind the best published PbS QD solar cells with 9.2% power conversion efficiency.[35]

Core−shell structures and overcoating of QD films have been investigated as a means to increase both the stability and transport properties in QD solids.[33,36−45] Recently, new synthetic strategies based upon Pb halide precursors improved the stability and resistance to ambient oxygen, leading to colloidal, air-stable PbSe QDs.[34,46,47] Zhang et al. first demonstrated that a $PbCl_2$−oleylamine complex as the Pb precursor resulted in PbSe QDs that were resistive to oxidation. PbSe QD solar cells could be fabricated in ambient conditions (rather than in an oxygen-free glovebox) and achieved a power conversion efficiency of ∼2%.[46] In a subsequent report the authors demonstrated further improvements by using a synthetic technique to first synthesize CdSe QDs of the desired size and then convert them to PbSe by a cation exchange reaction with the same $PbCl_2$−oleylamine complex. Solar cells fabricated in air from the resulting PbSe QDs produced a record power conversion efficiency of 6.2%.[34]

Inorganic and short molecular ligands (as small as single-atoms) are being explored as a means to improve the charge-carrier mobilities in QD films.[19,48−52] But, ligands also have a significant effect on the valence band position in QD films, which requires thoughtful design of devices made from new treatments.[3,4] Halide-based ligands and surface treatments show the deepest valence band positions of all the studied ligands and have been shown to enhance the air stability of QD films.[3,4,53] According to Ip et al. removing native ligands exposes trap states and the halide anions passivate those exposed states.[54] For example, Crisp et al. developed a PbI_2 surface treatment for PbS QD solar cells resulting in >7% efficient devices that are stable in ambient conditions.[4] Also, the five most recently published record reports for QD solar cells have employed halide passivation of PbS QDs to achieve high efficiencies.[35,53−56]

As with many solar cell technologies, a major limiter of QDSCs in general is the low open circuit voltage (V_{OC}) compared to the ideal V_{OC} for a given bandgap. Furthermore, the V_{OC} for PbSe QDSCs is lower than that of corresponding

Received: June 8, 2015
Accepted: July 7, 2015

DOI: 10.1021/acs.jpclett.5b01214
J. Phys. Chem. Lett. 2015, 6, 2892−2899

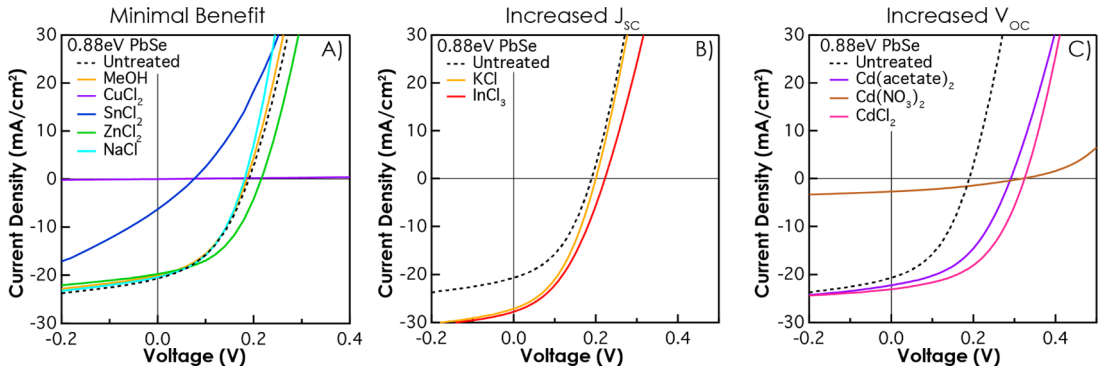

Figure 1. (a) J–V curves for treatments that had no effect or were detrimental to the device performance. (b) Two treatments, KCl and $InCl_3$, drastically improved the current density of devices, from 21 to 27 mA/cm^2 without reducing the V_{OC}. (c) J–V curves for the PbSe QD films treated in cadmium salts. All cadmium salts, regardless of the anion, increased the V_{OC} by at least 100 mV.

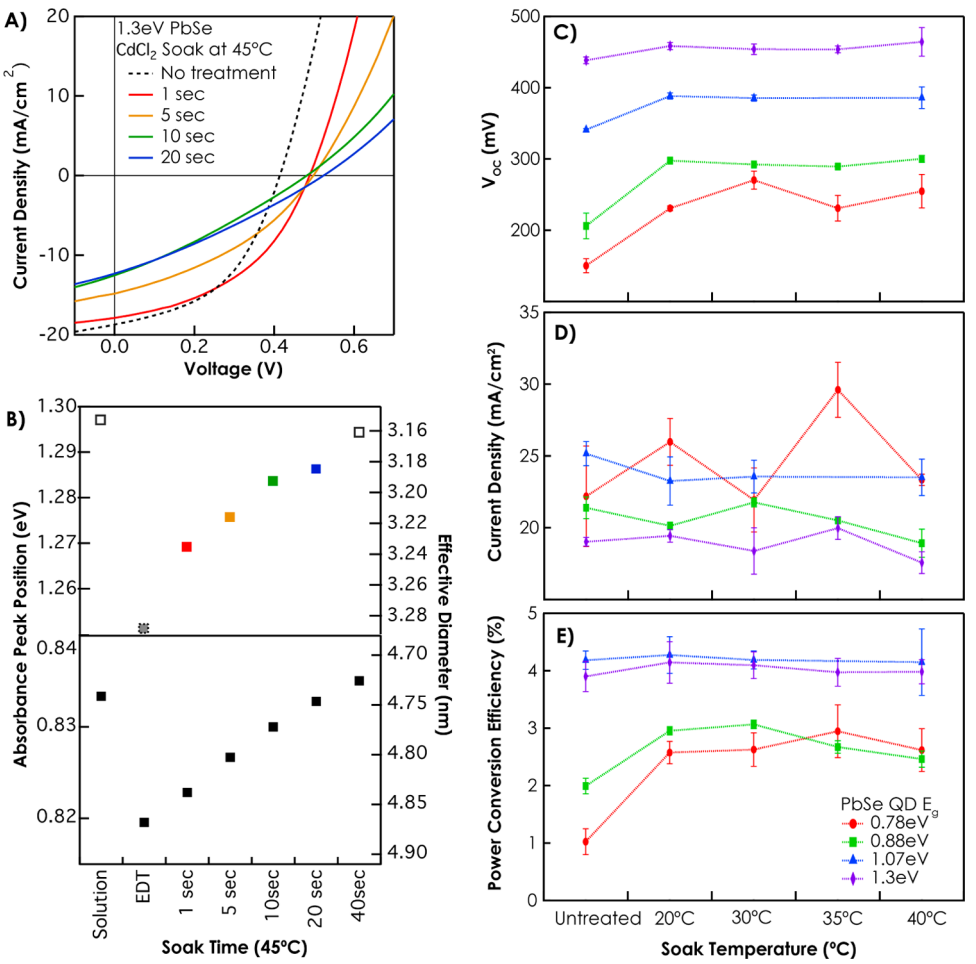

Figure 2. (a) All $CdCl_2$ treatments improved the V_{OC} over that of the untreated device, but longer soaks resulted in decreased current and increased series resistance. (b) 1S exciton peak position in original QD solution, in a film treated with EDT and as a function of $CdCl_2$ soak time for two different QD sizes. Top shows 3.2 nm PbSe with first exciton near 1.3 eV (color coded to match panel A) and bottom shows 4.8 nm PbSe with first exciton of 0.83 eV. (c) V_{OC}, (d) J_{SC}, and (e) power conversion efficiency as a function of $CdCl_2$ soak temperatures (1 s soak time) for QD films with bandgap ($E_{g\text{-}Abs}$) ranging from 0.78 to 1.3 eV.

bandgap PbS QD devices. The highest V_{OC} reported for PbSe is 520 mV, whereas PbS has achieved 655 mV with QDs of the same 1.3 eV bandgap.[34,57] Here, we show that using a combination of the cation-exchange synthesis and post-film processing metal halide treatments, we can utilize air-stable PbSe QDs, produce highly efficient devices at lower bandgap, and increase either the J_{SC} or V_{OC} by choice of treatment.

PbSe QD samples with various bandgaps ranging from 0.78 to 1.3 eV were synthesized according to Zhang et al. using a method based on cation exchange from CdSe.[34] Then, 400 nm thick, PbSe QD films were assembled onto TiO_2-coated F:SnO_2 by dipcoating using 1 mM 1,2-ethanedithiol (EDT) in acetonitrile to remove the native ligands. The key step for this work involves submersing the films in methanol (MeOH)

DOI: 10.1021/acs.jpclett.5b01214
J. Phys. Chem. Lett. 2015, 6, 2892–2899

saturated with metal salts, prior to evaporating the top contact, for various times and at various bath temperatures. A control device was soaked in neat MeOH to ensure that the solvent was not the cause of any changes in device performance observed.

Introducing metal impurities into nanocrystals can, in some cases, dope them *n*- or *p*-type depending on the charge state of the dopant.[58−62] Addition of metal impurities may also heal defect states. For example, Choi et al. showed that thermally diffusing In metal into a CdSe QD film resulted in band-like electronic transport, which they attributed to the filling of sub- and mid-gap defect states due to the incorporation of In into CdSe QDs.[61] Here, we developed a process of introducing metal cations along with halide anions by simply immersing the as-formed QD solids in a MeOH solution containing the dissolved metal halides. We studied the following metal salts: NaCl, $CuCl_2$, $SnCl_2$, $CdCl_2$, ZnCl, KCl, $InCl_3$, $Cd(acetate)_2$, and $Cd(NO_3)_2$. We chose metals with varying oxidation states (+1 to +3) and good solubility in MeOH. We find strong effects on optoelectronic properties of PbSe QD devices with certain treatments.

First, the PbSe QD films were soaked for 1 s in MeOH solutions at 45 °C. In Figure 1, the current−voltage characteristics of 0.88 eV PbSe QD solar cells are categorized into treatments that had minimal or detrimental effects (Figure 1a), treatments that improved the short circuit current density (J_{SC}) (Figure 1b), and treatments that enhanced the open circuit voltage (V_{OC}) (Figure 1c). NaCl and $ZnCl_2$ had little effect on the device performance, whereas $CuCl_2$ and $SnCl_2$ had detrimental effects. Both KCl and $InCl_3$ increased the short-circuit current while $CdCl_2$ increased the V_{OC} by over 100 mV (Figure 1b,c). Two nonhalide Cd^{2+} salts were explored ($Cd(acetate)_2$ and $Cd(NO_3)_2$), and from these studies we conclude that addition of Cd^{2+} increases the V_{OC}, but that the NO_3^- anion has a negative effect on overall performance by decreasing the current and fill factor (Figure 1c).

We find that of all the metal salts studied, $CdCl_2$ exhibits the most beneficial effects; therefore, we further explored $CdCl_2$ treatments. Using a bath temperature of 45 °C, the soak time was varied from 1 to 20 s (Figure 2a). We find an 80 mV increase in the V_{OC} after only 1 s of $CdCl_2$ treatment. Longer soak times cause a decrease in the J_{SC} and fill factor, which we attribute to the formation of transport barriers between QDs as too much Cd is incorporated into the PbSe film, and thus increasing series resistance in the device and limiting charge collection.

To support our assessment, the spectral position of the first exciton absorption peak for QDs with E_g of 1.3 (Figure 2b) and 0.8 eV (Figure 2c) continually blue shifts with treatment time. The peak position can be correlated to the core (PbSe) size of the QD and we use a previously published sizing curve to estimate the effective diameter of the PbSe QDs in the film;[63,64] the 1S peak position has also been used as a tool to determine the average core size in PbSe/CdSe core/shell QDs.[65] Initial formation of the film using EDT causes a redshift of 14 meV (for 0.8 eV QDs) and 45 meV (for 1.3 eV QDs) and is well documented in the literature.[12,21,41,66] As the $CdCl_2$ soak times increase, the peak position shows a general (but very slight) blue shift. Over a 40 s time window this blue shift is ∼15 meV for 1.3 eV QDs, corresponding to a change in effective diameter of only 1.3 Å (3.29 nm neat EDT film, to 3.16 nm after 40 s), which is much less than the thickness of one monolayer of Pb or Se. The larger, 0.8 eV PbSe QDs showed a similar effect with a change in effective diameter of 1.4 Å (4.87 nm neat EDT film, to 4.73 nm after 40 s, Figure 2b).

The minimal shift of the first exciton after a 1 s soak in $CdCl_2$ (3 meV) combined with the large increase in V_{OC} (∼100 mV) leads us to postulate that the Cd ions do not rapidly replace Pb, but first passivate specific QD surface sites. Pietryga et al. show significant spectral shifts when performing a cation exchange on the surface of PbSe QDs, even for shells <1 nm thick.[65] Comparing the spectral shifts measured in Figure 2 (using the $CdCl_2$ treatment) to this previous work, we do not have a complete CdSe shell forming during the first 1 s of treatment. After longer treatment times (or higher temperatures) the Cd will begin to replace Pb atoms at the surface, perhaps even forming a thin shell, which is a barrier to electronic transport and possibly explains the lower current in devices with long $CdCl_2$ treatment times.

We next studied the temperature of the soak treatments. Using the 1 s soak time, the temperature of the treatment was varied from 20 to 40 °C (Figure 2c−e). At the highest temperature, there is a decrease in J_{SC} for some devices, showing that higher temperatures promote fast ion-absorption in the film. The optimal temperature was 30 °C, where a small amount of Cd was incorporated, improving the V_{OC} without a deleterious loss in current. The effect of EDT and $CdCl_2$ ligands on the valence band energy level in PbS QDs coincidentally leads to similar energy levels.[3,4] Therefore, we postulate that the addition of $CdCl_2$ to the EDT treated film should not alter the valence band or Fermi level energies. Hence, the V_{OC} enhancement is not a result of a larger bandgap or shifting energy levels in the film, but more likely from trap passivation at the QD surface.

The V_{OC} gains are more pronounced for lower bandgap samples, and thus the optimization of the $CdCl_2$ treatment results in the highest efficiency PbSe QD devices reported to date for low-bandgap films (below 1.1 eV, Figure 3b). Note that we use the peak of the lowest energy exciton in the solution absorption spectrum to estimate the bandgap of the QDs ($E_{g\text{-}Abs}$) and to inform about the physical size of the QD. However, the bandgap of films in solar cells are generally determined using a Tauc plot (details in the Supporting Information). As an alternative to the 1S absorption feature, a recent publication estimated the bandgap of PbS QDSC using the onset of the EQE.[67] Using the EQE spectra to estimate the absorption of the films, we make a Tauc plot and find the x intercept of a linear fit to the low energy side in order to calculate the bandgap ($E_{g\text{-}EQE}$); this value is used to calculate theoretical performance parameters, as below in the discussion of V_{OC} deficit. The $E_{g\text{-}EQE}$ is always found to be lower in energy than the $E_{g\text{-}Abs}$; the four sizes studied here show $E_{g\text{-}EQE}$ of 0.73, 0.77, 0.93, and 1.1 eV for $E_{g\text{-}Abs}$ of 0.78, 0.88, 1.07, and 1.3 eV, respectively.

Recently, the large V_{OC} deficit in QDSCs has been acknowledged as a major limiting factor in overall power conversion efficiency and likely results from trap-assisted recombination.[68,69] Given the large increase in V_{OC} with the Cd-based soak treatment presented in this work, we show the percentage of the theoretical V_{OC} (using the Shockley−Queisser formalism)[70] achieved in devices before and after the $CdCl_2$ treatment (Figure 3). The $CdCl_2$ treatment reduces the V_{OC} deficit by as much as 20%, most significantly for the lower bandgap material (larger diameter PbSe QDs), and represents a promising approach to improving the performance of QDSCs.

DOI: 10.1021/acs.jpclett.5b01214
J. Phys. Chem. Lett. 2015, 6, 2892−2899

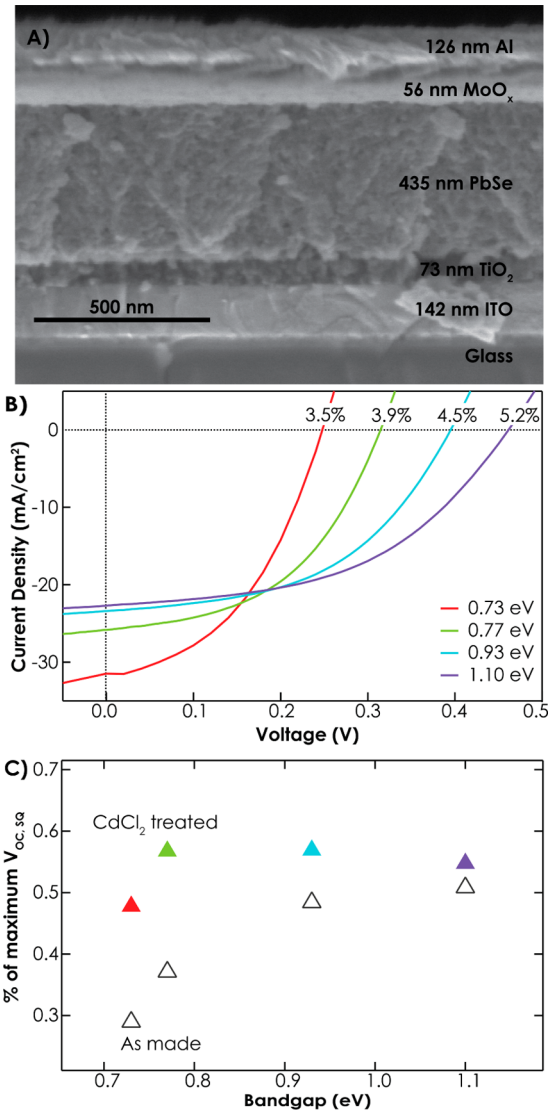

Figure 3. (a) Scanning electron microscopy (SEM) image showing the cross section of a typical PbSe QD device. (b) $J-V$ curves for the top performing devices with $E_{g\text{-}EQE}$ = 0.73 to 1.1 eV fabricated using the 1 s, 30 °C, $CdCl_2$ treatment. (c) V_{OC} deficit calculated as a percentage of the maximum theoretical V_{OC} using the Shockley Queisser analysis for each film's $E_{g\text{-}EQE}$. The untreated devices are shown as open triangles and the $CdCl_2$-soaked films are shown as colored triangles matching the legend in panel B. The $CdCl_2$ treated devices reach a higher percentage of the maximum allowable V_{OC}.

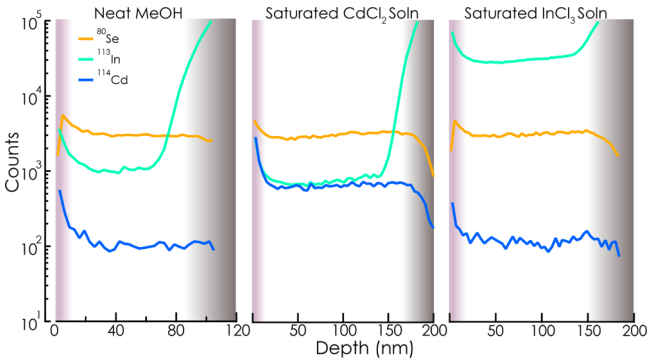

Figure 4. Secondary ion mass spectrometry (SIMS) shows the ^{113}In, ^{114}Cd, and ^{80}Se signals from three treated films. The absolute counts were normalized by the ^{80}Se signal. The methanol rinse (left) is the reference for a neat QD film. The film treated with $CdCl_2$ (middle) shows a substantial and uniform increase in the amount of ^{114}Cd detected by SIMS throughout the thickness of the film. The $InCl_3$ treated film likewise shows a uniform increase in the ^{113}In signal (right). The surface of the film is shaded in purple and the gray shading indicates the ITO layer below the PbSe QD film. The ^{113}In signal increases and other signals begin to decrease once the ITO layer is reached. The bulk of the QD film is represented by the unshaded region.

Secondary-ion mass spectrometry (SIMS) and inductively coupled plasma mass spectrometry (ICP-MS) were used to assess the cadmium and indium incorporation of the treated PbSe films. Films were dipcoated using EDT in the same manner as described for device fabrication, then the films were exposed to either neat MeOH, or saturated MeOH solutions of $CdCl_2$ or $InCl_3$. In Figure 4, we show the depth-dependent SIMS profile for the measured Se, In, and Cd content. The In signal in the $InCl_3$ treated film is 2 orders of magnitude higher than in the MeOH and $CdCl_2$ treated films, and similarly the relative amount of Cd in the $CdCl_2$ treated film is an order of magnitude higher than in the MeOH or $InCl_3$ treated film. These results demonstrate that a 1 s soak in a salt solution results in significant incorporation of the metal cation evenly throughout the entire thickness of the QD solid. The ICP samples were prepared by digesting the treated films in nitric acid. The ICP data (Supporting Information) is in agreement with the SIMS and shows clear indication of Cd and In uptake by the films upon the 1 s soak.

The Cd content was also measured using SIMS as a function of immersion time in the $CdCl_2$ solution. $CdCl_2$ treated films show a 5-fold increase in the amount of Cd. The difference in Cd content between the different time soaks is not noticeable within the sensitivity of the SIMS measurement, but the 1S absorption peak continues to shift (as shown in Figure 2b) and long treatment times lead to reduced transport. This implies that the initial immersion quickly incorporates Cd into the film, passivating trap states on the QD surfaces and causing the increase in V_{OC}. An excess of Cd limits transport though, as seen in the J_{SC} decrease for long treatment times and elevated bath temperatures.

Halide treatments have been shown in many cases to provide QDs with protection from oxidative attack.[47,71,72] We find that chloride post-treatments (specifically $CdCl_2$ and $InCl_3$) improve the air stability of devices. The $InCl_3$ device shows better air stability than an untreated device (Figure 5, blue triangles, especially apparent around days 10–20). $CdCl_2$ shows the best air stability overall (Figure 5). We attribute this stability to the passivation of the surface: Cd fills defect states,[73] leading to an improved V_{OC}, whereas Cl lowers the work function[3,4] making the films resistive to oxidation. Comparing these devices to one treated with $Cd(acetate)_2$ (Supporting Information Figure S1), we can see the effect of Cd without Cl: the V_{OC} increase is apparent from Figure 1 and the air stability is enhanced slightly from the untreated case. However, the device completely degrades between 5 and 27 days, more similar to the $InCl_3$ treated device than the $CdCl_2$ treatment. The copassivation of Cd and Cl in the device results in PbSe QDSCs that can be stored in air for over 270 days and maintain ~80% of their initial efficiency.

We report on the inclusion of metal and halide ions, post-film fabrication, as a means of enhancing the efficiency of low bandgap PbSe QDSCs by simply exposing QD solids to metal

DOI: 10.1021/acs.jpclett.5b01214
J. Phys. Chem. Lett. 2015, 6, 2892–2899

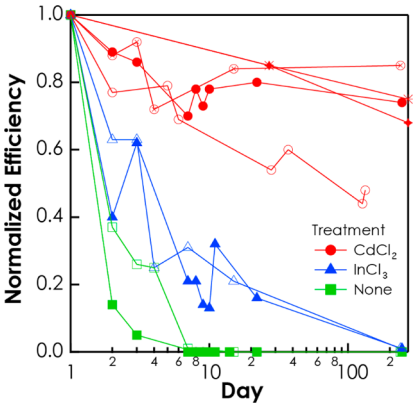

Figure 5. Efficiency of multiple devices is graphed as a function of days after fabrication while being stored in air, normalized to the efficiency on the first day. Devices with no chloride treatment (green squares) were not functional within the first few days of air exposure. The $InCl_3$ treatment (blue triangles) offers some protection; devices were still functional after almost a month in air, albeit less so than at the beginning and degraded to 0% under long-term air exposure. The $CdCl_2$ treatment (red circles) offered the best protection, losing little efficiency (in some cases <20% relative to initial values), even up to 270 days of air storage. Individual devices are denoted with different symbols and connecting lines.

halide solutions in MeOH. We find that $CdCl_2$ has the best enhancement. The addition of Cd drastically reduces the V_{OC} deficit by passivating limiting defects and the combination of Cd and Cl enhances the air stability of QDSCs. Larger diameter PbSe QDs show the most improvement from the $CdCl_2$ treatment. Devices are stored in air for over 270 days and retain close to 80% of the original efficiency. This work aids in the advancement of QDSCs by enabling air-stable, high efficiency PbSe devices, especially for low bandgap films, which are ideal for studying MEG in QD solar cells.

PbSe QD Synthesis. PbSe QDs were synthesized following a previously published procedure, through a cation exchange of CdSe QDs.[34] First, 0.834 g (3 mmol) of $PbCl_2$ (Sigma Alrich, 99.999%, reagent grade) is mixed in 10 mL (3 mmol) of oleylamine (OLA, Sigma-Aldrich, technical grade) and heated to 100 °C under vacuum. The mixture maintained at 100 °C for 5 min under flowing N_2, then heated to 140 °C for 30 min under N_2 to complex the $PbCl_2$ and OLA. The mixture is heated to the desired reaction temperature, depending on the target size for the PbSe NCs. Previously prepared CdSe NCs,[34] capped with Cd-oleate, in 1-octadecene (ODE, Sigma-Aldrich, technical grade) (50−100 mg/mL) are injected into the mixture, resulting in an immediate color change from red to black as the material converts from CdSe to PbSe. After 30 s, the reaction is quenched with a water bath. Once the reaction solution has cooled to room temperature, 8 mL of oleic acid (OA, Sigma-Aldrich, technical grade) is injected to replace the weakly bound OLA ligands on the surface of the PbSe. In order to synthesize different sizes of PbSe QDs, the following sizes (given as the first exciton peak in the absorption spectra) of CdSe and temperatures were used: 950 nm, 500 nm CdSe @ 140 °C; 1155 nm, 564 nm CdSe @ 160 °C; 1410 nm, 580 nm CdSe @ 190 °C; 1590 nm, 612 nm CdSe @ 195 °C. The NCs were washed two times using hexane/methanol (both from Sigma-Aldrich, reagent grade) as the solvent/antisolvent pair, then filtered and dispersed in hexane at ∼15 mg/mL for dipcoating.

TiO_2 Sol-Gel. The TiO_2 sol-gel is prepared by mixing 5 mL of anhydrous ethanol, 2 drops of hydrochloric acid, and 125 μL of deionized water. This mixture is stirred while 375 μL of titanium ethoxide (Sigma-Aldrich, ≥97%) is added dropwise to the solution. This forms a clear liquid and the vial headspace is filled with nitrogen. The solution is stirred for 48 h before storing in the freezer. The sol-gel is removed from the freezer 10 min before use and stirred at room temperature.

Photovoltaic Devices. Prepatterned ITO and FTO on glass are purchased from Thin Film Devices, with thicknesses of 150 and 200 nm, respectively. The substrates are cleaned vigorously with ethanol and a stream of air is used to remove any dust. The TiO_2 layer is fabricated in two steps starting with a sol-gel layer spun at 1400 rpm for 30 s. This layer is annealed at 115 °C for 30 min and at 450 °C for 30 min. After the films have cooled, TiO_2 NPs dispersed in ethanol are spun at 1400 rpm for 30 s and undergo a similar annealing process (115 °C for 30 min and 450 °C for 20 min). The films are kept in air overnight before use. The QD layer is fabricated using a layer-by-layer dipcoating process that has been outlined previously in the literature.[74] PbSe QDs are dipcoated from hexane with 1 mM 1,2-ethanedithiol in acetonitrile to remove the native ligand; approximately 20 layers results in 250−350 nm thick films.

This film is then treated with a saturated $CdCl_2$ solution in MeOH (∼25 mg/mL) at various temperatures. The film is soaked in the $CdCl_2$/MeOH solution for 1 s then washed thoroughly with reagent grade isopropanol. The films are annealed on a hot plate at 111 °C in the glovebox for 20 min before the evaporation of 20−50 nm molybdenum trioxide and 200 nm aluminum. This completes the full device stack of FTO/TiO_2/PbSe QDs/MoO_x/Al. The devices were always stored in air while the EQE and $J-V$ curves were acquired in an oxygen-free environment.

ICP-MS. PbSe QD films were dipcoated using 1 mM EDT on glass substrates, then 1 s treatments were done at 30 °C in neat MeOH, $CdCl_2$, and $InCl_3$. The films were dissolved in 70% HNO_3 in water, trace metals basis. The solutions were then diluted with water (trace metals basis) and HNO_3 to make solutions of 5 vol % HNO_3 in water. The samples were submitted to the Laboratory for Environmental and Geological Studies (LEGS) at the University of Colorado, Boulder, for ICP-MS analysis.

Secondary Ion Mass Spectrometry (SIMS). Films were dipcoated in a manner mimicking device fabrication (without the TiO_2 layer) for SIMS analysis. PbSe QDs in hexane (15 mg/mL) and 1 mM EDT in acetonitrile were used to dipcoat a film 200 nm thick onto an ITO substrate. MeOH and metal chloride soak treatments were done for 1 s with the solutions at 35 °C. The films were analyzed in a Cameca IMS 5f instrument with a Cs^+ primary ion beam and positive secondary ions.

■ ASSOCIATED CONTENT

Ⓢ Supporting Information

ICP-MS results, explanation of bandgap determination, a stability plot for a Cd-acetate treated device, and XRD data are included in the Supporting Information. This material is available free of charge via the Internet The Supporting Information is available free of charge on the ACS Publications website at DOI: 10.1021/acs.jpclett.5b01214.

■ AUTHOR INFORMATION

Corresponding Author

*E-mail: joey.luther@nrel.gov.

DOI: 10.1021/acs.jpclett.5b01214
J. Phys. Chem. Lett. 2015, 6, 2892−2899

Notes

The authors declare no competing financial interest.

■ ACKNOWLEDGMENTS

The authors would like to thank Bobby To for SEM images, Fredrick Luiszer for ICP measurements, and Nathan Neale for supplying TiO_2 nanoparticles. This work was supported by the U.S. Department of Energy Office of Science, Office of Basic Energy Sciences Energy Frontier Research Centers program within the Center for Advanced Solar Photophysics (CASP). DOE funding was provided to NREL through contract DE-AC36-08G028308.

■ REFERENCES

(1) Beard, M. C.; Luther, J. M.; Nozik, A. J. The Promise and Challenge of Nanostructured Solar Cells. *Nat. Nanotechnol.* **2014**, *9*, 951−954.

(2) Erslev, P. T.; Chen, H.-Y.; Gao, J.; Beard, M. C.; Frank, A. J.; van de Lagemaat, J.; Johnson, J. C.; Luther, J. M. Sharp Exponential Band Tails in Highly Disordered Lead Sulfide Quantum Dot Arrays. *Phys. Rev. B: Condens. Matter Mater. Phys.* **2012**, *86*, 155313.

(3) Brown, P. R.; Kim, D.; Lunt, R. R.; Zhao, N.; Bawendi, M. G.; Grossman, J. C.; Bulović, V. Energy Level Modification in Lead Sulfide Quantum Dot Thin Films through Ligand Exchange. *ACS Nano* **2014**, *8*, 5863−5872.

(4) Crisp, R. W.; Kroupa, D. M.; Marshall, A. R.; Miller, E. M.; Zhang, J.; Beard, M. C.; Luther, J. M. Metal Halide Solid-State Surface Treatment for High Efficiency PbS and PbSe QD Solar Cells. *Sci. Rep.* **2015**, *5*, 9945.

(5) Zhang, J.; Crisp, R. W.; Gao, J.; Kroupa, D. M.; Beard, M. C.; Luther, J. M. Synthetic Conditions for High-Accuracy Size Control of PbS Quantum Dots. *J. Phys. Chem. Lett.* **2015**, *6*, 1830−1833.

(6) Hughes, B. K.; Luther, J. M.; Beard, M. C. The Subtle Chemistry of Colloidal, Quantum-Confined Semiconductor Nanostructures. *ACS Nano* **2012**, *6*, 4573−4579.

(7) Semonin, O. E.; Luther, J. M.; Choi, S.; Chen, H.-Y.; Gao, J.; Nozik, A. J.; Beard, M. C. Peak External Photocurrent Quantum Efficiency Exceeding 100% via MEG in a Quantum Dot Solar Cell. *Science* **2011**, *334*, 1530−1533.

(8) Padilha, L. A.; Stewart, J. T.; Sandberg, R. L.; Bae, W. K.; Koh, W.-K.; Pietryga, J. M.; Klimov, V. I. Carrier Multiplication in Semiconductor Nanocrystals: Influence of Size, Shape, and Composition. *Acc. Chem. Res.* **2013**, *46*, 1261−1269.

(9) Beard, M. C.; Luther, J. M.; Semonin, O. E.; Nozik, A. J. Third Generation Photovoltaics Based on Multiple Exciton Generation in Quantum Confined Semiconductors. *Acc. Chem. Res.* **2013**, *46*, 1252−1260.

(10) Trinh, M. T.; Houtepen, A. J.; Schins, J. M.; Hanrath, T.; Piris, J.; Knulst, W.; Goossens, A. P. L. M.; Siebbeles, L. D. A. In Spite of Recent Doubts Carrier Multiplication Does Occur in PbSe Nanocrystals. *Nano Lett.* **2008**, *8*, 1713−1718.

(11) Ellingson, R. J.; Beard, M. C.; Johnson, J. C.; Yu, P.; Micic, O. I.; Nozik, A. J.; Shabaev, A.; Efros, A. L. Highly Efficient Multiple Exciton Generation in Colloidal PbSe and PbS Quantum Dots. *Nano Lett.* **2005**, *5*, 865−871.

(12) Luther, J. M.; Beard, M. C.; Song, Q.; Law, M.; Ellingson, R. J.; Nozik, A. J. Multiple Exciton Generation in Films of Electronically Coupled PbSe Quantum Dots. *Nano Lett.* **2007**, *7*, 1779−1784.

(13) Midgett, A. G.; Hillhouse, H. W.; Hughes, B. K.; Nozik, A. J.; Beard, M. C. Flowing versus Static Conditions for Measuring Multiple Exciton Generation in PbSe Quantum Dots. *J. Phys. Chem. C* **2010**, *114*, 17486−17500.

(14) Shabaev, A.; Hellberg, C. S.; Efros, A. L. Efficiency of Multiexciton Generation in Colloidal Nanostructures. *Acc. Chem. Res.* **2013**, *46*, 1242−1251.

(15) Midgett, A. G.; Luther, J. M.; Stewart, J. T.; Smith, D. K.; Padilha, L. A.; Klimov, V. I.; Nozik, A. J.; Beard, M. C. Size and Composition Dependent Multiple Exciton Generation Efficiency in PbS, PbSe, and PbS_xSe_{1-x} Alloyed Quantum Dots. *Nano Lett.* **2013**, *13*, 3078−3085.

(16) Schaller, R. High Efficiency Carrier Multiplication in PbSe Nanocrystals: Implications for Solar Energy Conversion. *Phys. Rev. Lett.* **2004**, *92*, 186601.

(17) Wang, H.; Pei, Y.; LaLonde, A. D.; Snyder, G. J. Heavily Doped P-Type PbSe with High Thermoelectric Performance: An Alternative for PbTe. *Adv. Mater.* **2011**, *23*, 1366−1370.

(18) Zhou, J.; Yang, R. Quantum and Classical Thermoelectric Transport in Quantum Dot Nanocomposites. *J. Appl. Phys.* **2011**, *110*, 084317.

(19) Hetsch, F.; Zhao, N.; Kershaw, S. V.; Rogach, A. L. Quantum Dot Field Effect Transistors. *Mater. Today* **2013**, *16*, 312−325.

(20) Leschkies, K. S.; Kang, M. S.; Aydil, E. S.; Norris, D. J. Influence of Atmospheric Gases on the Electrical Properties of PbSe Quantum-Dot Films. *J. Phys. Chem. C* **2010**, *114*, 9988−9996.

(21) Liu, Y.; Gibbs, M.; Puthussery, J.; Gaik, S.; Ihly, R.; Hillhouse, H. W.; Law, M. Dependence of Carrier Mobility on Nanocrystal Size and Ligand Length in PbSe Nanocrystal Solids. *Nano Lett.* **2010**, *10*, 1960−1969.

(22) Padilha, L. A.; Stewart, J. T.; Sandberg, R. L.; Bae, W. K.; Koh, W.-K.; Pietryga, J. M.; Klimov, V. I. Aspect Ratio Dependence of Auger Recombination and Carrier Multiplication in PbSe Nanorods. *Nano Lett.* **2013**, *13*, 1092−1099.

(23) Luther, J. M.; Law, M.; Beard, M. C.; Song, Q.; Reese, M. O.; Ellingson, R. J.; Nozik, A. J. Schottky Solar Cells Based on Colloidal Nanocrystal Films. *Nano Lett.* **2008**, *8*, 3488−3492.

(24) Ma, W.; Swisher, S. L.; Ewers, T.; Engel, J.; Ferry, V. E.; Atwater, H. A.; Alivisatos, A. P. Photovoltaic Performance of Ultrasmall PbSe Quantum Dots. *ACS Nano* **2011**, *5*, 8140−8147.

(25) Hoye, R. L. Z.; Ehrler, B.; Böhm, M. L.; Muñoz-Rojas, D.; Altamimi, R. M.; Alyamani, A. Y.; Vaynzof, Y.; Sadhanala, A.; Ercolano, G.; Greenham, N. C.; et al. Improved Open- Circuit Voltage in ZnO−PbSe Quantum Dot Solar Cells by Understanding and Reducing Losses Arising from the ZnO Conduction Band Tail. *Adv. Energy Mater.* **2014**, *4*, 1301544.

(26) Ko, D.-K.; Brown, P. R.; Bawendi, M. G.; Bulović, V. P-I-N Heterojunction Solar Cells with a Colloidal Quantum-Dot Absorber Layer. *Adv. Mater.* **2014**, *26*, 4845−4850.

(27) Kuo, C.-Y.; Su, M.-S.; Hsu, Y.-C.; Lin, H.-N.; Wei, K.-H. An Organic Hole Transport Layer Enhances the Performance of Colloidal PbSe Quantum Dot Photovoltaic Devices. *Adv. Funct. Mater.* **2010**, *20*, 3555−3560.

(28) Kuo, C.-Y.; Su, M.-S.; Ku, C.-S.; Wang, S.-M.; Lee, H.-Y.; Wei, K.-H. Ligands Affect the Crystal Structure and Photovoltaic Performance of Thin Films of PbSe Quantum Dots. *J. Mater. Chem.* **2011**, *21*, 11605−11612.

(29) Ma, W.; Luther, J. M.; Zheng, H.; Wu, Y.; Alivisatos, A. P. Photovoltaic Devices Employing Ternary PbS_xSe_{1-X} Nanocrystals. *Nano Lett.* **2009**, *9*, 1699−1703.

(30) Ouyang, J.; Schuurmans, C.; Zhang, Y.; Nagelkerke, R.; Wu, X.; Kingston, D.; Wang, Z. Y.; Wilkinson, D.; Li, C.; Leek, D. M.; et al. Low-Temperature Approach to High-Yield and Reproducible Syntheses of High-Quality Small-Sized PbSe Colloidal Nanocrystals for Photovoltaic Applications. *ACS Appl. Mater. Interfaces* **2011**, *3*, 553−565.

(31) Dai, Q.; Wang, Y.; Zhang, Y.; Li, X.; Li, R.; Zou, B.; Seo, J.; Wang, Y.; Liu, M.; Yu, W. W. Stability Study of PbSe Semiconductor Nanocrystals over Concentration, Size, Atmosphere, and Light Exposure. *Langmuir* **2009**, *25*, 12320−12324.

(32) Chappell, H. E.; Hughes, B. K.; Beard, M. C.; Nozik, A. J.; Johnson, J. C. Emission Quenching in PbSe Quantum Dot Arrays by Short-Term Air Exposure. *J. Phys. Chem. Lett.* **2011**, *2*, 889−893.

(33) Liu, Y.; Gibbs, M.; Perkins, C. L.; Tolentino, J.; Zarghami, M. H.; Bustamante, J.; Law, M. Robust, Functional Nanocrystal Solids by Infilling with Atomic Layer Deposition. *Nano Lett.* **2011**, *11*, 5349−5355.

DOI: 10.1021/acs.jpclett.5b01214
J. Phys. Chem. Lett. 2015, 6, 2892−2899

(34) Zhang, J.; Gao, J.; Church, C. P.; Miller, E. M.; Luther, J. M.; Klimov, V. I.; Beard, M. C. PbSe Quantum Dot Solar Cells with More than 6% Efficiency Fabricated in Ambient Atmosphere. *Nano Lett.* **2014**, *14*, 6010−6015.
(35) Labelle, A. J.; Thon, S. M.; Masala, S.; Adachi, M. M.; Dong, H.; Farahani, M.; Ip, A. H.; Fratalocchi, A.; Sargent, E. H. Colloidal Quantum Dot Solar Cells Exploiting Hierarchical Structuring. *Nano Lett.* **2015**, *15*, 1101−1108.
(36) McDaniel, H.; Fuke, N.; Makarov, N. S.; Pietryga, J. M.; Klimov, V. I. An Integrated Approach to Realizing High-Performance Liquid-Junction Quantum Dot Sensitized Solar Cells. *Nat. Commun.* **2013**, *4*, 2887.
(37) Shen, Q.; Kobayashi, J.; Diguna, L. J.; Toyoda, T. Effect of ZnS Coating on the Photovoltaic Properties of CdSe Quantum Dot-Sensitized Solar Cells. *J. Appl. Phys.* **2008**, *103*, 084304.
(38) Liu, C.; Mu, L.; Jia, J.; Zhou, X.; Lin, Y. Boosting the Cell Efficiency of CdSe Quantum Dot Sensitized Solar Cell via a Modified ZnS Post-Treatment. *Electrochim. Acta* **2013**, *111*, 179−184.
(39) Mora-Seró, I.; Giménez, S.; Fabregat-Santiago, F.; Gómez, R.; Shen, Q.; Toyoda, T.; Bisquert, J. Recombination in Quantum Dot Sensitized Solar Cells. *Acc. Chem. Res.* **2009**, *42*, 1848−1857.
(40) Ihly, R.; Tolentino, J.; Liu, Y.; Gibbs, M.; Law, M. The Photothermal Stability of PbS Quantum Dot Solids. *ACS Nano* **2011**, *5*, 8175−8186.
(41) Liu, Y.; Tolentino, J.; Gibbs, M.; Ihly, R.; Perkins, C. L.; Liu, Y.; Crawford, N.; Hemminger, J. C.; Law, M. PbSe Quantum Dot Field-Effect Transistors with Air-Stable Electron Mobilities above 7 $cm^2 V^{-1} s^{-1}$. *Nano Lett.* **2013**, *13*, 1578−1587.
(42) Ten Cate, S.; Liu, Y.; Suchand Sandeep, C. S.; Kinge, S.; Houtepen, A. J.; Savenije, T. J.; Schins, J. M.; Law, M.; Siebbeles, L. D. A. Activating Carrier Multiplication in PbSe Quantum Dot Solids by Infilling with Atomic Layer Deposition. *J. Phys. Chem. Lett.* **2013**, *4*, 1766−1770.
(43) Peng, X.; Schlamp, M. C.; Kadavanich, A. V.; Alivisatos, A. P. Epitaxial Growth of Highly Luminescent CdSe/CdS Core/Shell Nanocrystals with Photostability and Electronic Accessibility. *J. Am. Chem. Soc.* **1997**, *119*, 7019−7029.
(44) Cirloganu, C. M.; Padilha, L. A.; Lin, Q.; Makarov, N. S.; Velizhanin, K. A.; Luo, H.; Robel, I.; Pietryga, J. M.; Klimov, V. I. Enhanced Carrier Multiplication in Engineered Quasi-Type-II Quantum Dots. *Nat. Commun.* **2014**, *5*, 4148.
(45) Zhang, Y.; Dai, Q.; Li, X.; Cui, Q.; Gu, Z.; Zou, B.; Wang, Y.; Yu, W. W. Formation of PbSe/CdSe Core/Shell Nanocrystals for Stable Near-Infrared High Photoluminescence Emission. *Nanoscale Res. Lett.* **2010**, *5*, 1279−1283.
(46) Zhang, J.; Gao, J.; Miller, E. M.; Luther, J. M.; Beard, M. C. Diffusion-Controlled Synthesis of PbS and PbSe Quantum Dots with in Situ Halide Passivation for Quantum Dot Solar Cells. *ACS Nano* **2014**, *8*, 614−622.
(47) Zhang, Z.; Liu, C.; Zhao, X. Utilizing Sn Precursor To Promote the Nucleation of PbSe Quantum Dots with in Situ Halide Passivation. *J. Phys. Chem. C* **2015**, *119*, 5626−5632.
(48) Kim, S.; Noh, J.; Choi, H.; Ha, H.; Song, J. H.; Shim, H. C.; Jang, J.; Beard, M. C.; Jeong, S. One-Step Deposition of Photovoltaic Layers Using Iodide Terminated PbS Quantum Dots. *J. Phys. Chem. Lett.* **2014**, *5*, 4002−4007.
(49) Crisp, R. W.; Panthani, M. G.; Rance, W. L.; Duenow, J. N.; Parilla, P. A.; Callahan, R.; Dabney, M. S.; Berry, J. J.; Talapin, D. V.; Luther, J. M. Nanocrystal Grain Growth and Device Architectures for High-Efficiency CdTe Ink-Based Photovoltaics. *ACS Nano* **2014**, *8*, 9063−9072.
(50) Kovalenko, M. V.; Scheele, M.; Talapin, D. V. Colloidal Nanocrystals with Molecular Metal Chalcogenide Surface Ligands. *Science* **2009**, *324*, 1417−1420.
(51) Nag, A.; Chung, D. S.; Dolzhnikov, D. S.; Dimitrijevic, N. M.; Chattopadhyay, S.; Shibata, T.; Talapin, D. V. Effect of Metal Ions on Photoluminescence, Charge Transport, Magnetic and Catalytic Properties of All-Inorganic Colloidal Nanocrystals and Nanocrystal Solids. *J. Am. Chem. Soc.* **2012**, *134*, 13604−13615.
(52) Talapin, D. V.; Lee, J.-S.; Kovalenko, M. V.; Shevchenko, E. V. Prospects of Colloidal Nanocrystals for Electronic and Optoelectronic Applications. *Chem. Rev.* **2010**, *110*, 389−458.
(53) Ning, Z.; Voznyy, O.; Pan, J.; Hoogland, S.; Adinolfi, V.; Xu, J.; Li, M.; Kirmani, A. R.; Sun, J.-P.; Minor, J.; et al. Air-Stable N-Type Colloidal Quantum Dot Solids. *Nat. Mater.* **2014**, *13*, 822−828.
(54) Ip, A. H.; Thon, S. M.; Hoogland, S.; Voznyy, O.; Zhitomirsky, D.; Debnath, R.; Levina, L.; Rollny, L. R.; Carey, G. H.; Fischer, A.; et al. Hybrid Passivated Colloidal Quantum Dot Solids. *Nat. Nanotechnol.* **2012**, *7*, 577−582.
(55) Tang, J.; Kemp, K. W.; Hoogland, S.; Jeong, K. S.; Liu, H.; Levina, L.; Furukawa, M.; Wang, X.; Debnath, R.; Cha, D.; et al. Colloidal-Quantum-Dot Photovoltaics Using Atomic-Ligand Passivation. *Nat. Mater.* **2011**, *10*, 765−771.
(56) Chuang, C.-H. M.; Brown, P. R.; Bulović, V.; Bawendi, M. G. Improved Performance and Stability in Quantum Dot Solar Cells through Band Alignment Engineering. *Nat. Mater.* **2014**, *13*, 796−801.
(57) Yoon, W.; Boercker, J. E.; Lumb, M. P.; Placencia, D.; Foos, E. E.; Tischler, J. G. Enhanced Open-Circuit Voltage of PbS Nanocrystal Quantum Dot Solar Cells. *Sci. Rep.* **2013**, *3*, 2225.
(58) Liu, H.; Zhitomirsky, D.; Hoogland, S.; Tang, J.; Kramer, I. J.; Ning, Z.; Sargent, E. H. Systematic Optimization of Quantum Junction Colloidal Quantum Dot Solar Cells. *Appl. Phys. Lett.* **2012**, *101*, 151112.
(59) Sahu, A.; Kang, M. S.; Kompch, A.; Notthoff, C.; Wills, A. W.; Deng, D.; Winterer, M.; Frisbie, C. D.; Norris, D. J. Electronic Impurity Doping in CdSe Nanocrystals. *Nano Lett.* **2012**, *12*, 2587−2594.
(60) Stavrinadis, A.; Rath, A. K.; de Arquer, F. P. G.; Diedenhofen, S. L.; Magén, C.; Martinez, L.; So, D.; Konstantatos, G. Heterovalent Cation Substitutional Doping for Quantum Dot Homojunction Solar Cells. *Nat. Commun.* **2013**, *4*, 2981.
(61) Choi, J.-H.; Fafarman, A. T.; Oh, S. J.; Ko, D.-K.; Kim, D. K.; Diroll, B. T.; Muramoto, S.; Gillen, J. G.; Murray, C. B.; Kagan, C. R. Bandlike Transport in Strongly Coupled and Doped Quantum Dot Solids: A Route to High-Performance Thin-Film Electronics. *Nano Lett.* **2012**, *12*, 2631−2638.
(62) Luther, J. M.; Pietryga, J. M. Stoichiometry Control in Quantum Dots: A Viable Analog to Impurity Doping of Bulk Materials. *ACS Nano* **2013**, *7*, 1845−1849.
(63) Moreels, I.; Lambert, K.; De Muynck, D.; Vanhaecke, F.; Poelman, D.; Martins, J. C.; Allan, G.; Hens, Z. Composition and Size-Dependent Extinction Coefficient of Colloidal PbSe Quantum Dots. *Chem. Mater.* **2007**, *19*, 6101−6106.
(64) Smith, D. K.; Luther, J. M.; Semonin, O. E.; Nozik, A. J.; Beard, M. C. Tuning the Synthesis of Ternary Lead Chalcogenide Quantum Dots by Balancing Precursor Reactivity. *ACS Nano* **2011**, *5*, 183−190.
(65) Pietryga, J. M.; Werder, D. J.; Williams, D. J.; Casson, J. L.; Schaller, R. D.; Klimov, V. I.; Hollingsworth, J. A. Utilizing the Lability of Lead Selenide to Produce Heterostructured Nanocrystals with Bright, Stable Infrared Emission. *J. Am. Chem. Soc.* **2008**, *130*, 4879−4885.
(66) Beard, M. C.; Midgett, A. G.; Law, M.; Semonin, O. E.; Ellingson, R. J.; Nozik, A. J. Variations in the Quantum Efficiency of Multiple Exciton Generation for a Series of Chemically Treated PbSe Nanocrystal Films. *Nano Lett.* **2009**, *9*, 836−845.
(67) Chuang, C.-H. M.; Maurano, A.; Brandt, R. E.; Hwang, G. W.; Jean, J.; Buonassisi, T.; Bulović, V.; Bawendi, M. G. Open-Circuit Voltage Deficit, Radiative Sub-Bandgap States, and Prospects in Quantum Dot Solar Cells. *Nano Lett.* **2015**, *15*, 3286−3294.
(68) Bozyigit, D.; Lin, W. M. M.; Yazdani, N.; Yarema, O.; Wood, V. A Quantitative Model for Charge Carrier Transport, Trapping and Recombination in Nanocrystal-Based Solar Cells. *Nat. Commun.* **2015**, *6*, 6180.
(69) Miller, O. D.; Yablonovitch, E.; Kurtz, S. R. Strong Internal and External Luminescence as Solar Cells Approach the Shockley-Queisser Limit. *IEEE J. Photovolt.* **2012**, *2*, 303−311.

DOI: 10.1021/acs.jpclett.5b01214
J. Phys. Chem. Lett. 2015, 6, 2892−2899

(70) Shockley, W.; Queisser, H. J. Detailed Balance Limit of Efficiency of P-n Junction Solar Cells. *J. Appl. Phys.* **1961**, *32*, 510−519.
(71) Bae, W. K.; Joo, J.; Padilha, L. A.; Won, J.; Lee, D. C.; Lin, Q.; Koh, W.; Luo, H.; Klimov, V. I.; Pietryga, J. M. Highly Effective Surface Passivation of PbSe Quantum Dots through Reaction with Molecular Chlorine. *J. Am. Chem. Soc.* **2012**, *134*, 20160−20168.
(72) Woo, J. Y.; Ko, J.-H.; Song, J. H.; Kim, K.; Choi, H.; Kim, Y.-H.; Lee, D. C.; Jeong, S. Ultrastable PbSe Nanocrystal Quantum Dots via in Situ Formation of Atomically Thin Halide Adlayers on PbSe(100). *J. Am. Chem. Soc.* **2014**, *136*, 8883−8886.
(73) Greaney, M. J.; Couderc, E.; Zhao, J.; Nail, B. A.; Mecklenburg, M.; Thornbury, W.; Osterloh, F. E.; Bradforth, S. E.; Brutchey, R. L. Controlling the Trap State Landscape of Colloidal CdSe Nanocrystals with Cadmium Halide Ligands. *Chem. Mater.* **2015**, *27*, 744−756.
(74) Luther, J. M.; Law, M.; Song, Q.; Perkins, C. L.; Beard, M. C.; Nozik, A. J. Structural, Optical, and Electrical Properties of Self-Assembled Films of PbSe Nanocrystals Treated with 1,2-Ethanedithiol. *ACS Nano* **2008**, *2*, 271−280.

DOI: 10.1021/acs.jpclett.5b01214
J. Phys. Chem. Lett. 2015, 6, 2892−2899